Papers

Relationships between atmospheric positive electric charge densities and gas bubble concentrations in the Baltic Sea

OCEANOLOGIA, 46 (4), 2004.
pp. 459–476.

KEYWORDS
Atmospheric electricity
Air ions
Gas bubbles
Baltic Sea

Zygmunt Klusek[1,*]
Andrzej Wiszniewski[2]
Jaromir Jakacki[3]

[1] Institute of Oceanology,
Polish Academy of Sciences,
Powstańców Warszawy 55, PL–81–712 Sopot, Poland;

e-mail: klusek@iopan.gda.pl

*corresponding author

[2] Medical University of Gdańsk,
Dębinki 1, PL–80–211 Gdańsk, Poland

[3] Naval Postgraduate School,
833 Dyer Road, Monterey, CA 93943, USA

Manuscript received 6 May 2004, reviewed 27 August 2004, accepted 28 October 2004.

Abstract

Simultaneous measurements of bubble density in the sea subsurface and positive ions in the lower atmosphere were performed in the Baltic Sea in the summer of 1999. Bubbles in two size ranges, around 27 and 100 μm, were measured acoustically. Airborne positive charge was measured with a Gerdien instrument. Observed concentrations of air ions varied from 60 cm^{-3} up to 600 cm^{-3}.

The relative role of bubbles and wind speed on the positive air ion concentrations over the brackish water of the Baltic Sea is discussed. The parameters of a model of a log-log dependence between charge concentration and bubble density are calculated.

The correlation functions between time series of concentrations of positive charges over the sea and gas bubbles averaged over a depth range from 0.4 to 4 m and wind speed are presented. There was zero lag between the cross-correlation maxima of charge and bubbles, but there was a phase lag of one and a half hours between charge and wind speed.

1. Introduction

In spite of the long history of investigations into atmospheric electrical phenomena over the Ocean (e.g. Parkinson & Torreson 1931, Gathman & Trent 1968), our knowledge of the relations between atmospheric electricity, weather and air pollution is insufficient. It is generally accepted from Blanchard's pioneering measurements (Blanchard 1955, 1963) that gas bubbles bursting at the water surface are the source of positively charged spray. Atmospheric charge measurements made at sea have confirmed the hypothesis that there is a close dependence between wind-produced whitecaps and space charge density (Gathman & Trent 1968). These researchers demonstrated that the concentration of atmospheric electricity is related to sea wave height, which in turn is correlated with the bubble generation intensity via surface wave breaking. However, Gathman & Trent reached one more conclusion in their publication, namely, that a correlation exists between charge and wind only over a certain range of wind speeds.

In the literature, the charge vs bubble correlation is regarded as one of the most obvious, but the formulae describing the dependence of charge concentration on bubble density are not known. The reason for this situation is that at the time when this problem attracted the most sustained interest, techniques for measuring gas bubble concentrations *in situ* did not exist. Unfortunately, in the literature one will still not find many parallel measurements of electrical charge concentration in the atmosphere and bubble density in the subsurface sea layers. Now, advances in bubble counting methods have made it possible to obtain reliable, digitally recorded and processed data and therefore to have a closer look at the dependence between charge and bubble concentration. It was these circumstances that provided the stimulus for the present work, the aim of which was to explain the part played by gas bubbles in the surface layer of the sea in the build-up of electrical charge in the atmosphere. We demonstrate that there is a correlation between charge concentration and wind speed, and between charge and bubble density. We will also show that there is a time lag, not only between ion charge density and wind speed, but also between bubble density and wind speed.

Charge production by drops ejected from air bubbles bursting at the water surface and bubble generation both depend on the salinity. Indeed, it is a known fact that salt concentration and ionic surfactants modify the charge characteristics of air bubbles (Iribarne & Mason 1967, Reiter 1994).

The reader's attention is drawn to the fact that the results presented here were obtained in sea water of a salinity (7 PSU) lower than that of oceanic water.

In addition to the marine air ion concentration, wind speed, water temperature and bubble concentrations were measured.

The paper is organised into three sections. The problem has been formulated in this introduction. The methods of gathering and processing bubble/charge data are described in Section 2, and the basic results are given in Section 3. The correlation and parameters of the dependence between positive space charge and wind speed/bubble population are discussed in Section 4. The conclusions are presented in Section 5.

2. Instrumentation and measurements (methods)

The investigations were carried out at oceanographic station P1 in the Gulf of Gdańsk (Baltic Sea). P1 is located at $\phi = 54°50.2'$N, $\lambda = 019°18.5'$E, at a minimal distance of 22 NM from the nearest land (Fig. 1 shows a map of the area). Two series of measurements of charge density in the atmosphere and bubble population in the seawater, performed in parallel,

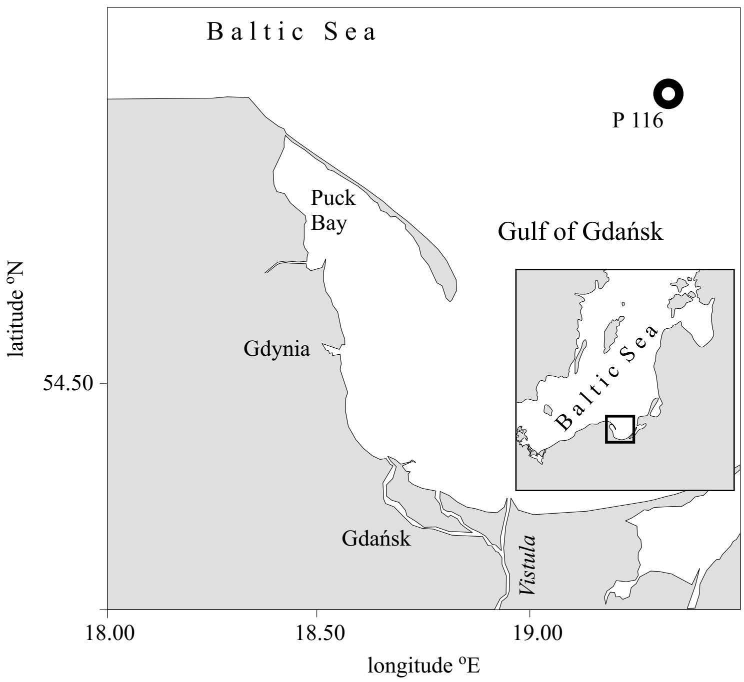

Fig. 1. Map of the study area

were undertaken in two summer seasons (1997 and 1999). In the first one, only negative ions and bubbles were recorded. However, during 105 hours of measurements, winds were no stronger than Force 2 B and negative ion densities obeyed the quasi-harmonic law with diurnal periods. The data reported below were collected in the second series of bubble density and positive charge measurements. They began at 18.00 on 21st August 1999 and continued until 18.00 on 25th August (local summer time), from the anchored research vessel 'Oceania'. Fifteen hours later, measurements of the bubble population started. So, in the following statistical analysis the subset of data from the first 15 hours of charge measurements is omitted from the correlation estimation. There was no rain or fog during the experiment.

2.1. Atmospheric charge density measurements

Atmospheric charge was measured using a Gerdien cylinder instrument. Originally designed to measure the conductivity of the air, the Gerdien method is now widely used to measure the density of air ions. The set-up used in charge concentration measurements was one of a series constructed by the Institute of Nuclear Physics in Kraków. The idea of the measurements involves measuring the flow of ions suspended in air and those deposited on the highly insulated electrode in the centre of the cylinder. The recorded voltage at resistor R relates to the number of ions per unit volume of air. The atmospheric air with charged particles flows through slits between a set of coaxial cylinders with controlled electric potentials between them. The slits calm the turbulent inflow of air at the input of the instrument. The ion's trajectory is deflected in the electrostatic field towards the axis of the cylinder (Fig. 2). Depending on its velocity, mass and charge, a charged particle is or is not deposited on the electrode, which allows its mobility to be determined. The air pumped from outside the ship entered the instrument chamber at the rate of 6.25×10^{-4} m^3 s^{-1}. The relatively high inlet flow rate, the large diameter of the chamber (12 cm), and

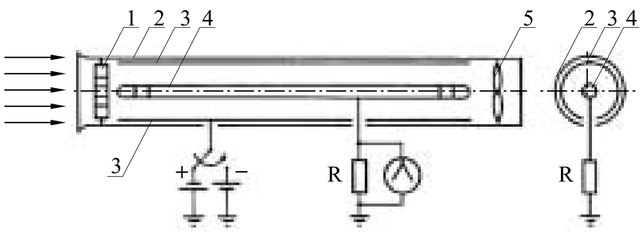

Fig. 2. Diagram of the Gerdien type instrument used in the measurements of charge density. 1 – inlet net, 2 – outer cylinder, 3 – outer electrode, 4 – central inner electrode, 5 – air fan

length of the electrode (32 cm) allowed us to reduce signal fluctuations, to obtain a greater sensitivity and to record charged particles over a relatively wide spectrum of ion mobility. The electric potential was selected in such a way that heavy, positive ions of relatively low mobility were measured from connected segments of the electrode. The ion mobility did not exceed the limiting value $\mu < 1.5\ 10^{-9}\ \mathrm{m}^2\ \mathrm{V}^{-1}\ \mathrm{s}^{-1}$ (the mobility of ions measured in meters squared per volt per second: this is the velocity that an ion will reach when exposed to a force in an electric field of one volt per meter). The experimental set-up used in our observations allowed only singly charged particles to be recorded during the whole experiment.

The atmospheric air inlet of the instrument was placed at a height of about 2 m above the sea surface, and horizontally displaced by about 2 m from the spot where the acoustic set-up was suspended in the water. The ship was oriented at an approximately constant angle to the wind direction. The charge density measurements were continuously registered by analogue recorder and sampled from the graph at the same time as bubble measurements were being made.

2.2. Bubble population measurements

The acoustic methods used to measure the bubble population during the experiment have become recognised as a standard tool in physical oceanography (Leighton 1997) and the disadvantages of the different variants of acoustic techniques are well recognised (Leighton et al. 1996). Since the method, apparatus and the validity of the technique used by our team has been analysed in detail before (Jakacki 2002) and presented at a hydroacousticians forum (Klusek & Jakacki 1998), it will be described in only very brief outline here.

Gas bubbles are effective acoustic scatterers at their resonant frequency (Medwin 1983) and, because of their broad size spectrum, resonant bubbles can be simply detected by acoustically active methods operating from about 10 kHz to around 100 kHz. The approximate resonant frequency of a bubble in water in kilohertz, according to Minnaert's formula (Leighton 1997)

$$f_R = \frac{3.27}{a_0}\sqrt{1 + 0.1\,z} \tag{1}$$

depends on the bubble radius a_0 (here in mm) and the depth z (in m) of the bubble in the water column. By measuring the echo intensity of the scattered signal, we could in principle calculate the number of bubbles at resonance with the sounding frequency in the insonified volume.

In the case of lower frequencies in the above range and where densities of plankton and fish are low, the echo intensity is proportional only to the number of bubbles at resonance with the sounding wave frequency and the intensity of the incident signal. But, in the presence of plankton layers, the echo from bubbles could be overwhelmed by the signal scattered by biological targets (zooplankton and small fishes). Working at higher frequencies we come across the problem of strong additional non-resonant scattering at the largest bubbles. So in order to avoid the influence of backscattering from non-resonant bubbles and biological targets the detection of the non-linear response of a bubble insonified with high-intensity acoustic pulses was proposed. This means that when water containing bubbles is acoustically sampled at frequency f, the signal scattered from the bubbles is found to contain harmonics of primary frequency i.e. $2f$, $3f$ and possibly higher. The sampling could also be performed using pulses at two adjacent frequencies. Then, in the scattered signal we observe a set of non-linear components beyond the harmonics of primary frequencies, components with difference $|f_1 - f_2|$ and sum $|f_1 + f_2|$ frequencies, the latter having the larger amplitude. Only bubbles excited at resonance generate the non-linear components of the echo signal at the sum and difference frequencies. This method is based on the theory of the non-linear response of a damped single gas bubble in a liquid medium at resonance frequency to a high-intensity sound (Sutin et al. 1998). Despite the fact that different linear and non-linear methods were used to detect and count the bubbles with radii near 100 μm and 27 μm, the bubble concentrations obtained at the sum frequencies are used in further analysis.

In the measurements we used a set of calibrated echo sounders with acoustic beams pointing towards the sea surface. The instrument consisted of two pairs of acoustic transmitters working at frequencies 30 and 33 kHz (resonant bubble size near the sea surface $a \approx 100$ μm) or 105 and 115 kHz (resonant bubbles with size around $a \approx 27$ μm) and a wide-band hydrophone. The footprint diameter of the acoustic beam of each transducer at the sea surface was approximately 2 m at 30/33 kHz and 0.75 m at 105 and 115 kHz; the length of the transmitted pulse was 1.5 ms. The effective volume of the sounding (sampling volume) for the linear method and for 30 kHz varied from 0.6 m^3 at 5 m from the transducers to about 3.6 m^3 at a distance of 11 m, and for the non-linear sum frequency method varied from 0.3 to 0.8 m^3 respectively. The return signal was received with a 14-bit resolution data acquisition board performing the analogue to digital conversion at a maximum sampling rate of 533 kS s^{-1}.

The acoustic system was deployed from the ship by means of a crane down to 10–12 m depth. The output of bubble measurements was the mean profile of the bubble number in a unit volume of 1 m^3 with the radius bin equal to 1 μm around the resonant frequency. The bubble population was measured every 30 min. In each session, ultrasound pings sampled the water column at 1 sec intervals. Two series each consisting of 50 pings were recorded for each pair of frequencies. The mean vertical profiles of the bubble concentration were calculated after non-coherent averaging over 100 pings for each pair of frequencies. The bubble concentration profiles were recorded from 6 m below the sea surface up to a depth of 0.5 m. The distance the echo signal travelled to the sea surface was monitored on the basis of the echo return time from the sea surface.

2.3. Wind speed measurements

The wind speed was measured with an analogue anemometer placed at a height of 10 m above sea level. The wind speeds used in this analysis are the average of 4 consecutive measurements (each on a time scale of 100 s). The data given below were obtained under moderate winds at $U_{10} < 10.5$ m s^{-1}, where U_{10} is the wind speed at the standard height of 10 m.

The point of observation has the minimum wind fetch from the southwest (20 NM from the tip of the Hel Peninsula) and 22 NM from the southeast. So, it was assumed that the local anthropogenic air pollution in the Gdańsk area did not substantially affect our charge density measurements. The dominant winds were from the west and southeast, which meant that the wind field direction was generally from the neighbouring land than from the sea.

3. Data presentation

3.1. Wind speed and bubble concentration

The wind history during the bubble measurements is presented in Fig. 3 together with the logarithm of bubble concentrations in the subsurface layer from 0.4 to 2.4 m for bubbles with radii around $a = 100$ μm. The same figure also shows the changes in recorded positive charge density and the changes in wind direction. During the course of the measurements the wind at first fluctuated around 4 m s^{-1} blowing from the open sea, and then dropped to almost zero at about the 30th hour of the experiment. The wind velocity vector almost totally reversed direction after a period of calm. After some short gusts, the wind speed increased continually to 10 m s^{-1}, then dropped slowly, veering north. At the time of these recordings there were no sea- or land-breezes.

From *in situ* measurements in the Ocean it was found that for a wind speed above the whitecap threshold level (6–7 m s^{-1}) the density of subsurface bubbles can be approximated according to the generally accepted form (Hall 1989):

$$N(a,\, z) \propto a^{-n}\, U_{10}^{m} \exp(-z/L), \tag{2}$$

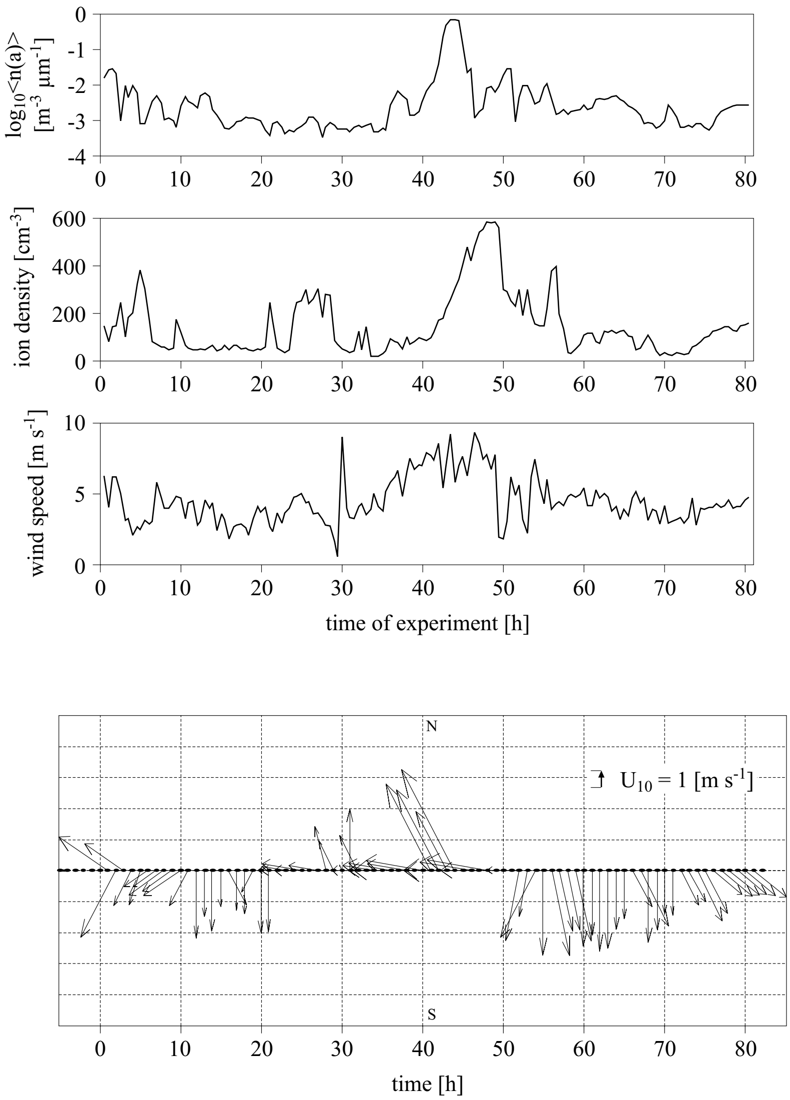

Fig. 3. Temporal variations in the logarithms of the averaged bubble concentration in the 0.4–2.4 m layer, positive charge density, and wind speed. The bubble radius is 100 μm. The wind directions recorded in one-hour periods are presented at the bottom

where U_{10} is the wind speed at 10 m above sea level, a – the bubble radius, z – the depth (positive downwards) and L – the bubble entrainment depth.

The concentration of gas bubbles $N(a,\, z)$ is the number of bubbles per unit volume per unit radius; the radius increment can be measured in meters or, as in this paper, in microns.

Beyond the above mentioned whitecap threshold level another wind speed threshold was expected due to the breaking of capillary waves. Small, unstable capillary waves turning over at a wind speed of about 3.5 m s^{-1} initiate bubble generation, which is reflected in the increase in the aerosol population. But in this process only a small number of bubbles appear in a thin layer, which are not transported/entrained deeper into the water body and were not detected by our method.

For depths ranging from the sea surface to $z = 3$ m, most experiments in the Ocean indicate values for n (in eq. (2)) of $3.5 < n < 5$, and for m from about 2.6 to as much as 4.5, depending on water salinity and temperature (e.g. Wu 1981, Haines & Johnson 1995).

It has also been found by many investigators that in fully developed sea waves, a constant layer of the smallest bubbles (of the order of 10 μm in size) independent of wind speed and wave height are present in all oceanic areas. This background layer is related to the previous sea state, to changes in water temperature or phytoplankton activity. Taking these facts into account, for both bubble size ranges investigated, eq. (2) for the mean bubble density in a layer can be written in another form:

$$N(a,\, z) = A\, U_{10}^{m} + B(a,\, z), \tag{3}$$

where $B(a, z)$ represents the wind-independent random component of the constant bubble layer in the surface water layer, and A is averaged over the bubble layer.

In our earlier investigations of the bubble population in the Baltic Sea, values of coefficient m were found to be dependent on the wind. In general, they were slightly lower in comparison to Ocean data. For example, during the four-day experiment performed in May 1995 with the same equipment, values of m in eq. (3) for wind speeds above 6 m s^{-1} were almost equal: for bubbles with a resonance frequency near 30 kHz – $m = 1.4$, and at 105 kHz $m = 1.8$.

Within the sampling volume, the fluctuation of bubble density from ping to ping recorded in an experiment could vary by as much as 3 orders of magnitude (especially at higher wind speeds), in particular, directly under the breaking wave. The very high, random fluctuations in bubble concentrations strongly influence the average bubble density over 100 pings in that the latter is encumbered with a large statistical error.

Employing the algorithm for fitting non-linear data to the formulae in the form given by eq. (3), we have found best-fit parameters of the bubble concentration in the water layer between 0.5–1 m versus wind speed. For bubbles of 100 μm size, this dependence was found in the form: $< n_{100\ \mu\mathrm{m}} >= 6.142 \times 10^{-6}\ U^{3.715} + 0.0006311$.

When the bubble data were grouped into two classes – the first one for wind speeds below the wave breaking threshold, and the second one for wind speeds $v > 6.5$ m s^{-1} – the values of m were found: for $U < 6.5$ m s^{-1}, $m = 0.6$ and for $U \geq 6.5$ m s^{-1}, $m = 3.4$.

3.2. Temporal variations in air ion density

Measurements of the positive charge density began 15 hours before the bubble estimation. However, Fig. 3 presents only the data from the time when the parallel bubble population measurements were made.

The background population of negative ions in the lower atmosphere over the land is usually independent of the state of the weather and varies in the range of 300–1000 elementary charges cm^{-3}. Positive ions are more abundant and exceed negative ions by 1.2–1.4 times. Similar values of positive ions were also registered during our measurements at sea.

Inspection of Fig. 3 and Fig. 7a shows clearly that charge density is wind-dependent, particularly in a rising wind. However, by grouping the charge data into two-hour bins and averaging them over all the days of the experiment, we also obtained a convincing picture of the periodic diurnal variations (Fig. 4). The diurnal fluctuations occurred repeatedly throughout the observation period.

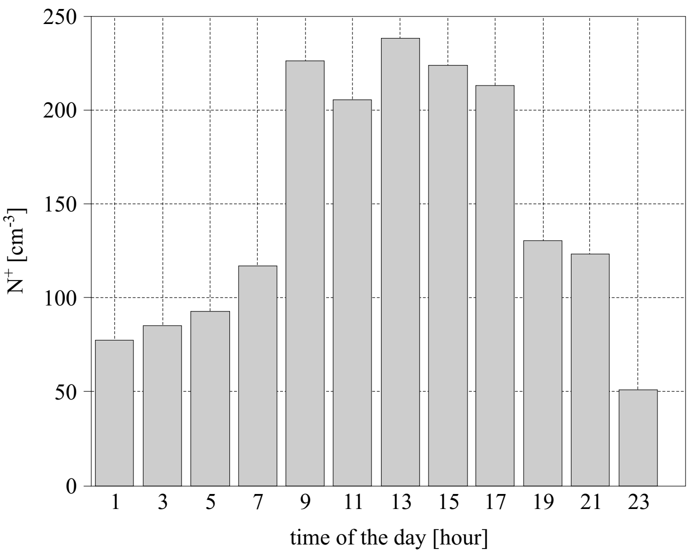

Fig. 4. Diurnal variations of the observed air ion density, averaged in two-hour bins. The data refer to the whole time when the ions were measured. The horizontal axis gives local summer time

The maximum space charge density was observed around midday. At night, the charge density decreased to about 1/4 of its peak daytime value, the level remaining almost constant from dusk to the late morning. The interesting feature of this diurnal oscillation is that the wind and bubble population did not behave in a similar way during this time. This last conclusion supports the calculated cross-spectra between charge and wind or bubbles, where we did not find any spectral peaks with the 24 h period.

4. Dependence of electric charge density on wind speed and bubble population

4.1. Cross correlation analysis

As was stated in Section 3, there is evidence in the time series of charge concentration that despite its diurnal changes, the positive atmospheric charge is related to the sea state parameters and the presence of bubbles via the so-called Blanchard effect (Blanchard 1955, 1963).

It is possible to discern some similarity between the charge concentration and the wind or bubble concentration curves. In the first step of the analysis, the covariance functions were estimated for time series of wind and bubbles, wind and charge, and charge and bubble concentrations.

According to the definition, the correlation and time delay between two time series X and Y can easily be found from the form and values of the covariance function, despite the high noise levels. The function is defined as the normalised unbiased mean cross-correlation

$$C_{XY}(k) = \begin{cases} \dfrac{1}{K-\mid k \mid} \displaystyle\sum_{n=0}^{K-|k|-1} (X_n - m_x)(Y_n - m_y) \quad \text{for} \quad k \geq 0 \\ C_{YX}(-k) \qquad \text{for} \quad k < 0, \end{cases} \tag{4}$$

where
K – length of series, $|k| < = 0.1\ K$.

In eq. (4) m_x, m_y, are the mean values of the time series X and Y respectively. This definition also includes the concept of the linear correlation coefficient r (in the sense of Pearson's r), that is, the correlation coefficient is the zero lag of the covariance function, and the successive C_{XY} terms are proportional to the linear correlation coefficient r from a series shifted by $m\,\Delta t$ (Δt – sampling period). In Fig. 3 we see that a really strong increase in charge density takes place when the wind speed exceeds the threshold value needed for whitecap production. The local ion concentration maxima are delayed when compared with the bubble population time series, which in turn are delayed when compared with the increasing or decreasing wind speed. In contrast to the bubble-wind dependence, we could see that the wind speed threshold for charge generation is somewhere above 3.5 m s^{-1}, when small capillary waves start breaking.

It is seen in Fig. 3 that the positive charge concentration shows a visible dependence on both wind speed and bubble concentration. The charge measured at a height of 2 m is the result of contributions from many wave breakers spread over a large area (the dependence is smoother if the ion detector is placed higher above the sea surface). It might therefore be expected that the correlation between wind speed and charge density field should be better than the charge-bubble correlation.

It should be noted here that in the time interval between the 22.5 and 27.7 hour of the data record, we observed similar changes in wind speed and charge concentration. At the same time there was no correlation between bubble density and wind. Of course, it is expected that the charge field will occasionally be contaminated by other sources, but in this case the passage of a front could have affected the results.

Fig. 5 shows the result of the covariance function between wind and charge performed on the data set presented in Fig. 3. Fig. 5 shows that there was a two-hour delay between the wind speed and the positive charge

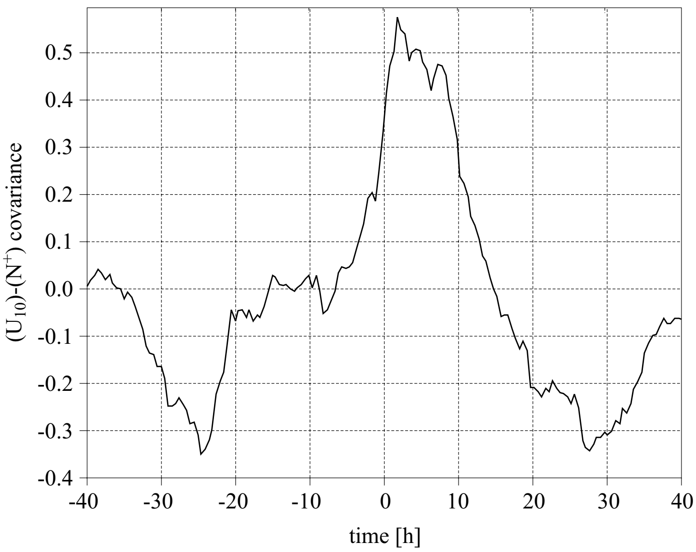

Fig. 5. The cross-covariance function between wind speed and ion concentration. The maximum positive values correspond to the charge and bubbles lagging the wind speed

concentrations. A similar time shift is seen for wind speed and bubble concentrations, but in the case of the larger bubbles, there are two peaks in the cross-covariance function: one with a zero time shift – the immediate response of the sea surface to wind gusts, the other with a lag of 3 hours – the delayed response to the breaking of fully developed waves.

The shape and width of the cross-covariance functions between wind and charge, and wind and bubble concentration around the peak are slightly different. In the case of the wind-charge correlation function, the curve around the peak is broadened. The correlation around the maximum tends to be slightly broader and the lag is inclined to be slightly greater for the wind-bubble dependence, an effect that must partly arise from the influence of the time when bubbles of different sizes are generated.

Another interpretation is that this difference is probably due to the different inertia time of the two processes. The bubble population decreases more quickly with the falling wind than air ions, which could be suspended in the air for a longer period of time. This reflects the fact that bubbles ($a > 100$ μm), newly formed as a result of Archimedes' buoyant force, are removed very quickly from the water body. This is true for all the largest bubbles (hundreds micrometers and more in size), which persist in the water only for as long as a wave period. The smallest fraction of bubbles with a diameter of the order of tens of microns, with their surface coated by surface-active substances preventing them from dissolving, could remain longer in the water body. Intensive dynamic processes in the sea transport them down from the sea surface both by random turbulence or convergent downwelling Langmuir convection, so that bubbles can remain in the seawater for a long time. Bursting at the surface and charge generation therefore continue for much longer. There is also a noticeable narrowing of the correlation function for wind and bubbles of one size, suggesting that at least some of the bubbles are born as a result of specific surface agitation.

In the case of the bubble-charge covariance function for larger bubbles, the covariance function has a maximum at the zero shift. However, a broader function with positive skewness is observed around the maximum. The generation of larger bubbles and positive ions are almost in phase. The behaviour of covariance is more complicated in the case of the dependence of smaller bubbles on positive air ions. There is a 1.5 h delay of air ions against small bubble concentration (Figs 6a and 6b). As yet, we have been unable to explain this effect.

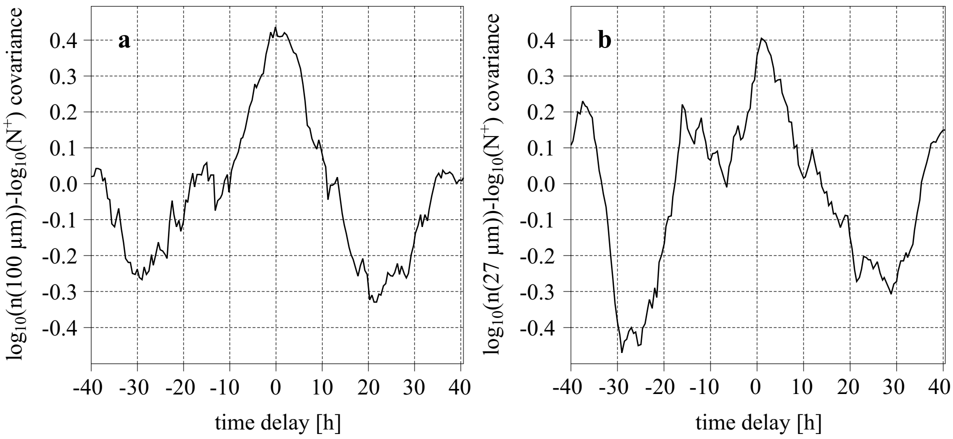

Fig. 6. Cross-covariance functions between the logarithm of ion concentration and the logarithm of bubble concentration 100 μm radius (a), and 27 μm radius (b)

4.2. Analysis of the dependence of air ion density on wind and bubbles

The power law dependence, identified earlier in the literature, between wind and bubble density (Wu 1981) and the mechanism of charge produced by bubbles (Blanchard 1955, 1963) suggests that a similar power law form of dependence could be proposed here. However, the observed wind-independent component of positive charge in the atmosphere and the constant background of the surface layer of bubbles also suggest a relationship in the form:

$$N^{(+)}(t) = b_1\, U_{10}^{m}(t+\tau) + b_0(t), \tag{5}$$

where b_0 is a charge component varying with time but functionally independent of the wind. One might suppose the changes in b_0 to be in some manner periodic and depend on the season and day of the year. This function is generally attributed to the exponential dependence of many natural sea surface processes on wind speed (among them, bubble production) but with some retardation – τ.

After mathematical transformations using the logarithms of both variables (wind and charge density, or wind and bubbles) and applying non-linear regression methods, the coefficients of regression were found. The data sets presented in Fig. 7a provide evidence in favour of the proposed form of the dependence. The figure also shows regression curves between charge (a) and bubbles (b) as functions of the local wind speed on a logarithmic scale that fits the data in a least-squares sense.

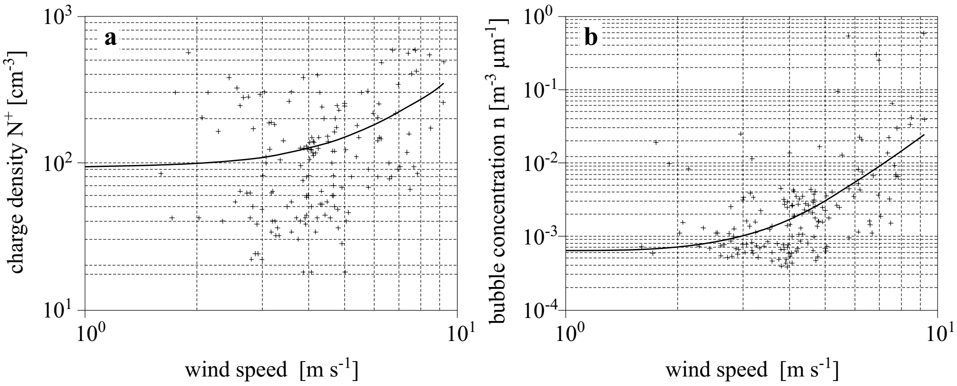

Fig. 7. Dependence of charge density in the atmosphere (a) and bubble concentration (b) with $a = 100$ μm averaged in the water 0.4–2.4 m layer on wind speed. No time shift between time series is used here for either the charge or the bubble-wind dependence

Note that in a low-wind-speed regime there is a higher variability of charge and bubble data in the log-log space. This is easily explained if we take into account the fact that in this area air pollution derived from the land can influence aerosol and marine air ion concentrations.

Using the same method as above when estimating the parameters of the non-linear wind-bubble relationship, we obtained parameters for the positive charge – wind dependence:

$$N^+ = 1.123\, U_{10}^{2.44} + 92.97,$$

where U_{10} is the wind speed in m s^{-1} at 10 m above sea leval.

In examining the charge-bubble dependence, the common linear regression technique was used to determine the linear relationships between the logarithm of the wind speed and the logarithm of charge, and between the logarithm of charge and that of the bubble concentration.

It was found that the linear regression coefficients relating the logarithms of charge density and the larger bubbles are

$$\log (N^+) = 0.25 \log (n_{a\,=\,100\ \mu\mathrm{m}}) + 2.74,$$

where $n_{a\,=\,100\ \mu\mathrm{m}}$ – the average concentration of bubbles of size 100 μm in unit volume (1 m^3) for the range of diameters da $= 1$ μm.

For smaller bubbles and for higher wind speeds $U_{10} > 6.5$ m s^{-1}, we have

$$\log (N^+) = 1.98 \log (n_{a\,=\,27\ \mu\mathrm{m}}) + 0.24.$$

To explore the consequence of the time lag, the charge data relating to measured wind speed, the significance of the Pearson r^2 correlation between the two linear data series was computed for different shifts with a time-step of half-an-hour. For estimating the wind-charge correlation, in the case of (U_{10}) – (N^+) pairs for all data, we have $r = 0.25$ for a zero time lag and a maximum value of $r = 0.54$ for a 1.5 h time shift (values of charge density are shifted backwards in time). Taking into account the mean concentration of bubbles, estimated in the water layer between $h = 0.4$ and 4 m for a 100 μm bubble radius, the correlation coefficient of the logarithms of bubble and charge concentrations for a zero time lag achieved a maximum value of $r = 0.45$.

The linear correlation coefficient for the log of the charge-small bubble concentration dependence (here about 30 μm in size) computed for a non-shifted time series was, at $r = 0.36$, slightly lower than the dependence between charge and larger bubbles.

It might be expected that a better correlation existed between charge and wind speed than between charge and bubble concentrations: our observations supported this. The moderate correlation of the charge concentration in relation to the bubble density could be due to several factors. First and foremost is the fact that the charge data at lower wind speeds reveals evidence of a significant contribution from wind-independent sources, biasing the estimated correlation coefficients. Secondly, the recorded bubble population is highly variable. We should remember that each bubble density data point represents a value averaged over 100 pings. A series averaged over 100 seconds could be too short to obtain an unbiased value. The charge-bubble correlation are rendered less precise because of the fact that the bubble concentration can vary by many orders of magnitude within a very short time. And finally, the relationship between charge and bubble density may not be simple or constant. Unfortunately, the measurements were not accompanied by the recording of other meteorological parameters, such as humidity, which can affect the presence of charge.

A bubble population measured locally (and for a short length of time) is influenced by wave breaking events and is subject to substantial and extremely brief fluctuations. The charge concentration measured at a given point is the result of contributions from many wave breakers – in other words, the outputs from sources spread over a wide area.

Thus, the surface of the cone in which bubbles were estimated within the footprint of the acoustic beam on the sea surface was around ten square meters centred over the set of transducers. In contrast, during the charge measurements, we analysed a mixed air sample originating from a relatively large source area of the sea surface: this area depended upon the inlet height of the electrometer, air turbulence and sea state. There was no reason to expect that a constant proportion between bubbles and charge should exist, even if bubbles were the only source of charge over the sea, which could explain the observed mismatch occurring in the statistical comparison of the time series presented above.

The outliers in Fig. 7(a–b) could be the manifestation of a phenomenon that is qualitatively different from the typical pattern of wind dependence and could provide evidence of a departure from the process of the charge generation by bursting bubbles.

5. Conclusions

On the basis of the results of our experiment we cannot establish a one-to-one relationship between the concentrations of air ions and bubbles. A non-linear regression technique was used to approximate the power law relationships between wind speed and positive charge in the atmosphere and between the charge and bubble concentrations. The covariance analysis of time series of charge and wind showed the retardation of the charge concentration and wind speed. The cross-correlation maximum between charge and bubbles occurred at or near zero lag, but that between charge and wind speed occurred with a phase lag of one and a half hours. While the correlation is quite low in the two bubble data sets, in every case the lag in the cross-correlation maxima has the same sign.

The most prominent feature is the appearance of a dependence of charge on both the wind speed and bubble density in accordance with a power law.

Positive space charge measurements exhibit a good correlation with wind speed and the bubble population, but this is due in part to the lack of measurements of many other parameters; little is known, for example, about vertical charge fluxes. The linear correlation coefficients between bubble and charge dependence, and between wind speed and charge are very close in value.

The fluctuations of charge density in light winds can probably be explained as follows: two processes moving in opposite directions are assumed to play the major role in affecting charge values over the sea surface – the flux of newly charged particles from bursting bubbles increasing with wind. On the other hand, it is possible that in lighter winds the charged particles of marine aerosols, for which the Coulombic forces prevent rapid precipitation, remain longer in the atmosphere. Also at such low wind speeds, surface processes that generate bubbles are not very active. We observe that with rising wind speeds, the charge density almost repeats the form of the wind speed changes.

Besides the charge-wind/bubble dependence there is also an indication of a consistent diel pattern in the positive ion concentrations above the sea surface.

Acknowledgements

The Institute of Oceanology, through the Marine Acoustics Programme, supported the participation in this study.

References

Blanchard D. C., 1955, *Electrified droplets from the bursting of bubbles at an air-sea water interface*, Nature, 175, 334.

Blanchard D. C., 1963, *The electrification of the atmosphere by particles from bubbles in the sea*, Prog. Oceanogr., 1, 72–202.

Gathman S., Trent E. M., 1968, *Space charge over the open ocean*, J. Atmos. Sci., 25 (6), 1075–1079.

Haines M. A., Johnson B. D., 1995, *Injected bubble populations in seawater and fresh water measured by a photographic method*, J. Geophys. Res., 100 (C4), 7057–7068.

Hall M. V., 1989, *A comprehensive model of wind generated bubbles in the ocean and predictions of the effects on the sound propagation at frequencies up to 40 kHz*, J. Acoust. Soc. Am., 86, 1103–1117.

Iribarne J. V., Mason B. J., 1967, *Electrification accompanying the bursting of bubbles in water and dilute aqueous solutions*, T. Faraday Soc., 63, 2234–2245.

Jakacki J., 2002, *Application of non-linear acoustic phenomena in investigations of gas bubbles in sea*, Ph. D. thesis, Inst. Oceanol. PAN, Sopot, (in Polish).

Klusek Z., Jakacki J., 1998, *Wind and time dependence of the gas bubble concentrations measured acoustically in the Baltic Sea*, Proc. 4th Europ. Conf. Underwater Acoust. (Rome), 107–112.

Leighton T. G., 1997, *The acoustic bubble*, Acad. Press, London, 640 pp.

Leighton T. G., Phelps A. D., Ramble D. G., Sharpe D. A., 1996, *Comparison of the abilities of eighth acoustic techniques to detect and size a simple bubble*, Ultrasonics, 34, 661–667.

Parkinson W. C., Torreson O. W., 1931, *The diurnal variation of the electric potential of the atmosphere over the oceans*, UGGI Bull., 8, 340–345.

Reiter R., 1994, *Charges on particles of different size from bubbles of Mediterranean Sea surf and from waterfalls*, J. Geophys. Res., 99 (D5), 10807–10812.

Sutin A. M., Yoon S. W., Kim E. J., Didenkulov I. N., 1998, *Non-linear acoustic method for bubble density measurements*, J. Acoust. Soc. Am., 103 (3), 2377 –2384.

Wu J., 1981, *Bubble populations and spectra in near-surface ocean: summary and review of field measurements*, J. Geophys. Res., 86, 457–463.